applied microbiology

MDPI

Article

MicroCT as a Useful Tool for Analysing the 3D Structure of Lichens and Quantifying Internal Cephalodia in *Lobaria pulmonaria*

Julia Gerasimova [1,2], Bernhard Ruthensteiner [3] and Andreas Beck [1,2,4,*]

1 Botanische Staatssammlung München, SNSB-BSM, D-80638 Munich, Germany; jgerasimova.lich@yandex.ru
2 Systematsche Botanik und Mykologie, University of Munich, D-80638 Munich, Germany
3 Zoologische Staatssammlung München, SNSB-ZSM, D-81247 Munich, Germany; ruthensteiner@snsb.de
4 GeoBio-Center, University of Munich, D-80333 Munich, Germany
* Correspondence: beck@snsb.de; Tel.: +49-89-1786-1266

Abstract: High-resolution X-ray computer tomography (microCT) is a well-established technique to analyse three-dimensional microstructures in 3D non-destructive imaging. The non-destructive three-dimensional analysis of lichens is interesting for many reasons. The examination of hidden structural characteristics can, e.g., provide information on internal structural features (form and distribution of fungal-supporting tissue/hypha), gas-filled spaces within the thallus (important for gas exchange and, thus, physiological processes), or yield information on the symbiont composition within the lichen, e.g., the localisation and amount of additional cyanobacteria in cephalodia. Here, we present the possibilities and current limitations for applying conventional laboratory-based high-resolution X-ray computer tomography to analyse lichens. MicroCT allows the virtual 3D reconstruction of a sample from 2D X-ray projections and is helpful for the non-destructive analysis of structural characters or the symbiont composition of lichens. By means of a quantitative 3D image analysis, the volume of internal cephalodia is determined for *Lobaria pulmonaria* and the external cephalodia of *Peltigera leucophlebia*. Nevertheless, the need for higher-resolution tomography for more detailed studies is emphasised. Particular challenges are the large sizes of datasets to be analysed and the high variability of the lichen microstructures.

Keywords: X-ray computer tomography; 3D image analysis; *Bacidia rubella*; *Evernia divaricata*; *Hypogymnia physodes*; *Lobaria pulmonaria*; *Peltigera leucophlebia*; *Xanthoria parietina*

Citation: Gerasimova, J.; Ruthensteiner, B.; Beck, A. MicroCT as a Useful Tool for Analysing the 3D Structure of Lichens and Quantifying Internal Cephalodia in *Lobaria pulmonaria*. *Appl. Microbiol.* **2021**, *1*, 189–200. https://doi.org/10.3390/applmicrobiol1020015

Academic Editor: Michael Lebuhn

Received: 20 May 2021
Accepted: 6 July 2021
Published: 13 July 2021

1. Introduction

The availability of non-destructive 3D examination technologies and increases in personal computer hardware and software enables various 3D graphical applications, such as surface visualisations of biological specimens. This approach indirectly recalled an old morphological method back to life, namely the investigation of soft part anatomy by a light microscopical serial section analysis [1]. The correlative examination of a small biological specimen offers many advantages in analysing, visualising, and validating results. The topographical correlation of high-resolution areas to the morphology of the whole specimen provides significant benefits for understanding the overall organisation of the sample [2].

Lichens comprise a large morphological diversity and appear as one organism, but in fact, they represent a symbiosis of at least two primary partners, a fungus (mycobiont) and an alga (photobiont), and many additional microorganisms of still unknown function [3–7]. In most cases, the fungal partner forms the major part and outer side of the lichen thallus and is often judged to be the predominant symbiont [8]. It positions the photoautotrophic algal partner in such a way to ensure optimal illumination and an increasing water supply while still facilitating a gas exchange, especially in the highly developed foliose and fruticose lichens. The mycobiont produces lichen secondary substances to protect the

photobiont against damage caused by high irradiation or UV light ([8–11] and references therein). The non-invasive determination of the internal morphology and anatomy of these fascinating life forms will help to understand their organisation and functioning better.

Species recognition has important implications for assessing the diversity and ecological and biogeographical patterns [12]. Based on phylogenetic and population studies, many cases have shown that numerous distinct lineages may be hidden under a single species name [12–18]. In these cases, microCT may be a beneficial tool, providing a complementation to other morphological examinations. It allows the visualisation and analysis of internal lichen microstructures, which could not be observed using routine light microscopy alone or can only be seen partially (with the need of preparing cross-sections).

In this proof of principle study, we intend to demonstrate the workflow for examining external and internal structures of lichens using datasets obtained from microCT. We used six samples of lichens from different genera and various growth forms: *Bacidia rubella* (Hoffm.) A. Massal., *Evernia divaricata* (L.) Ach., *Hypogymnia physodes* (L.) Nyl., *Lobaria pulmonaria* (L.) Hoffm., *Peltigera leucophlebia* (Nyl.) Gyeln., and *Xanthoria parietina* (L.) Th. Fr. The two lichens *Lobaria* and *Peltigera* have a green alga as the primary photobiont and incorporate nitrogen-fixing cyanobacteria into gall-like structures, the cephalodia. These are located either on the thallus surface (external cephalodia) or in its interior (internal cephalodia) [19]. Cephalodia have an essential ecological function: incorporated cyanobacteria fix atmospheric nitrogen, leading to a relatively high organic nitrogen content and, thus, enabling the colonisation of extremely oligotrophic habitats [9,20]. Consequently, these lichens contribute significant amounts of organic nitrogen to these ecosystems [21–23]. *Lobaria pulmonaria* is a tripartite lichen that contains the green alga *Symbiochloris reticulata* (Tschermak-Woess) Škaloud, Friedl, A. Beck & Dal Grande as the primary photobiont and *Nostoc* sp. in the internal cephalodia [24–27]. However, the structure and amount of these internal cephalodia are, so far, unknown. For this reason, we selected the internal and external cephalodia of *L. pulmonaria* and *P. leucophlebia*, respectively, for further analysis and quantification in this proof of principle study. The volumes of the segmented cephalodia of *L. pulmonaria* and *P. leucophlebia* relative to the size of the whole thallus were measured for the first time. Moreover, the shape and size of the internal cephalodia of *L. pulmonaria* were examined.

2. Materials and Methods

2.1. Taxon Sampling

We used six samples of lichens from different genera representing various growth forms: crustose, foliose, and fruticose (Table 1).

Table 1. Lichen samples used in this study with CT acquisition parameters and dataset details.

Name	Herbarium Number	Growth Form	Voxel Size (µm)	X, Y, and Z Voxel Dimensions of 8-Bit Datasets	Number of Projections	Duration of CT Acquisition
Bacidia rubella	M-0304302	crustose	1.24992	2085 × 1425 × 2262	1800	76 min
Evernia divaricata	M-0304299	fruticose	1.40618	1107 × 1332 × 2193	1700	71 min
Hypogymnia physodes	M-0304295	foliose	1.29594	2931 × 2875 × 2234	1800	90 min
Xanthoria parietina	M-0304310	foliose	1.65375	1104 × 2451 × 2298	1800	76 min
Lobaria pulmonaria	M-0304308	foliose	1.60658	2080 × 2290 × 2200	1800	76 min
Peltigera leucophlebia	M-0304309	foliose	1.61011	1901 × 2439 × 1820	1800	76 min

2.2. CT Acquisition

Lichen samples (Table 1) were stained with 1% iodine in 100% ethanol for approximately 24 h to enhance the contrast [28]. Dried lichen thalli were then directly glued with contact cement to a glass holder or put into a gelatin capsule glued to the glass holder. CT acquisition was performed with a Phoenix Nanotom M CT scanner (GE Measurement and Control, Wunstorf, Germany) using a voltage of 80 kV and a current of 325 mA while

using a tungsten ("standard") target. Projection images (1700–1800) were taken during a 360° rotation at a total duration ranging from 71 to 90 min. Voxel size ranged from 1.2 to 1.6 µm. The 16-bit dataset generated by reconstruction (with phoenix datos|x 2.2 software) was cropped and converted to 8 bit at a histogram adjustment prior to the other graphical processes.

2.3. Image Processing Using Amira Software

Data examination and analysis was performed using AMIRA® software v. 6.4 (Thermo Fisher Scientific, Hillsboro, OR, USA). It is a powerful, multifaceted software platform for visualising, manipulating, and understanding research data from many image modalities, including CT techniques [29]. The tools we applied are indicated in *italics* with a capital letter.

2.3.1. Visualisation of Lichen Structure Performed by *Volume Rendering* and *Clipping* Tools

We used *OrthoSlice* and *Volume Rendering* (*Volren*) modules to visualise the lichen image stack. *OrthoSlices* were combined with a specifically adapted *Grayscale Colormap* with standard grey values and a transparency function where the opacity can be set between 0 and 255. The adjustment of transparency allowed for the observation of internal lichen structures. The *Volren* module used for volume rendering provided a 3D visualisation of the whole sample dataset. The *Volren* module provided several options for adjustment: shaded and classical texture-based *Volume Rendering* (*VRT*), *Maximum Intensity Projection* (*MIP*), and *Digitally Reconstructed Radiograph* (*DRR*) (for more details, see reference [29]). To find the most appropriate one, we tested all the techniques and finally selected the option of *VRT*. Its virtual lighting effects enabled a better visualisation of fine details, which fit for our lichen objects best. The *Specular* lighting effect was enabled (Figures 1–4) as the most suitable for better visualisation of the thalli surface.

We applied the *Clipping* tool to examine the internal structures of the lichen thalli. We could quickly explore the data images by screening through multiple orthographic sections, which provided us with easy access and observation of the internal parts of lichen thalli. After *Clipping*, the *Volren* image (3D) was complemented with *OrthoSlices* (2D) for a better visualisation and examination of the internal surfaces (Figure 3).

2.3.2. Segmentation

Segmentation (separation of parts of the lichen tissue) was the most time-consuming step. It was mainly performed following the procedures outlined by Ruthensteiner [1], including a description and explanation of the *Segmentation* tools. A further detailed description of the applied techniques can be found in reference [29].

As an initial step of *Segmentation*, we applied *Thresholding* to separate the object (lichen tissue) from the background (air) by classifying the voxels into the foreground and background voxels based on their intensities or voxel values [29].

Segmentation of the internal and external lichen structures was performed manually (subjective decision), since we could not acquire an automated workflow. When trying automatic tools, some parts of interest were not included, or vice versa; the false attributes were labelled as well. Thus, at manual *Segmentation*, approximately every 10th section was labelled and followed by *Interpolation* to facilitate the segmentation process by obtaining relatively smooth material surfaces right away [1]. When necessary, we carried out additional correction steps by labelling missed parts followed by an *Interpolation* step until the complete labelling of the selected structure was achieved.

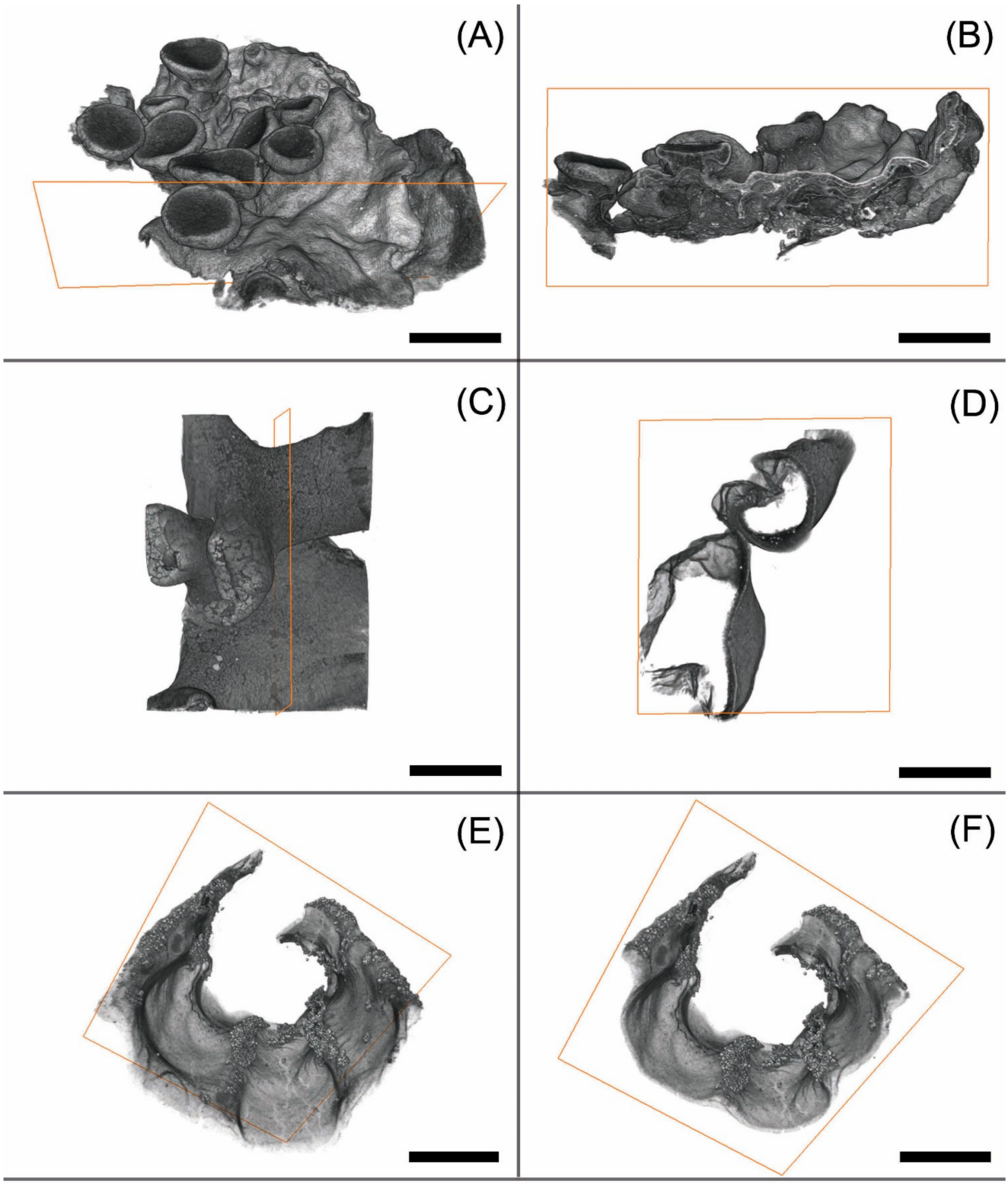

Figure 1. MicroCT renderings of lichen samples showing an overall view (**A**,**C**,**E**) and stratified thallus in a cross-section through the thallus (**B**,**D**,**F**) and apothecia (**B**), as provided by the *Clipping* tool. The orange rectangle indicates the cutting plane. (**A**,**B**) *Xanthoria parietina* (M-0304310), (**C**,**D**) *Hypogymnia physodes* (M-0304295), and (**E**,**F**) *Lobaria pulmonaria* (M-0304308). Scale: 1 mm (**A**,**B**,**E**,**F**) and 0.25 mm (**C**,**D**).

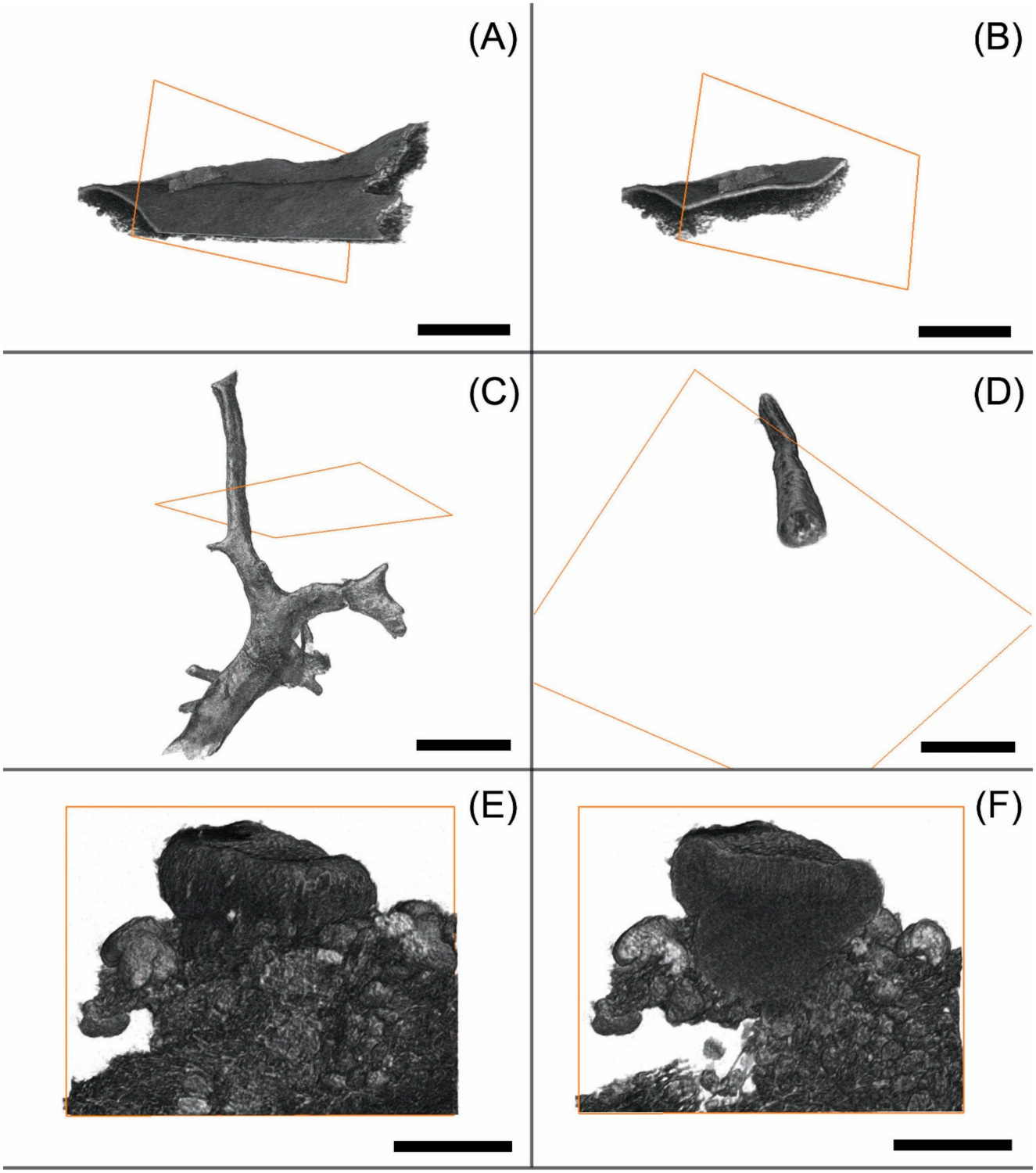

Figure 2. MicroCT renderings of lichen samples showing an overall view (**A**,**C**,**E**) and thalli in a cross-section (**B**,**D**,**F**) and apothecia (**F**), as provided by the *Clipping* tool. The orange rectangle indicates the cutting plane. (**A**,**B**) *Peltigera leucophlebia* (M-0304309), (**C**,**D**) *Evernia divaricata* (M-0304299), and (**E**,**F**) *Bacidia rubella* (M-0304302). Scale: 0.5 mm (**A**,**B**), 1 mm (**C**,**D**), and 0.25 mm (**E**,**F**).

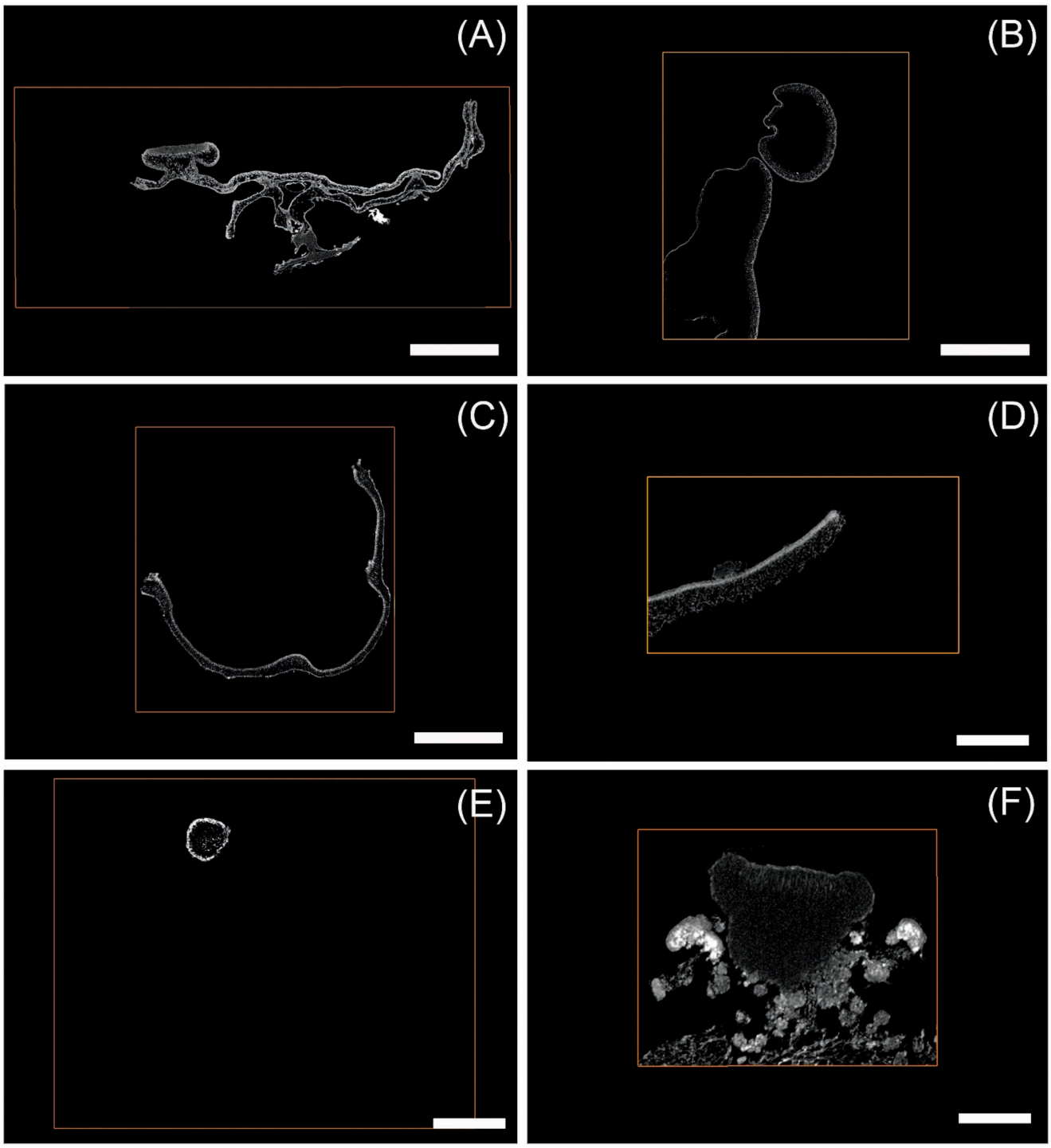

Figure 3. 2D *OrthoSlice* image sections, providing a view from the front (xy) of the cutting plane. (**A**) *Xanthoria parietina*, (**B**) *Hypogymnia physodes*, (**C**) *Lobaria pulmonaria*, (**D**) *Peltigera leucophlebia*, (**E**) *Evernia divaricata*, and (**F**) *Bacidia rubella*. Scale: 1 mm (**A**,**C**), 0.5 mm (**E**), and 0.25 mm (**B**,**D**,**F**).

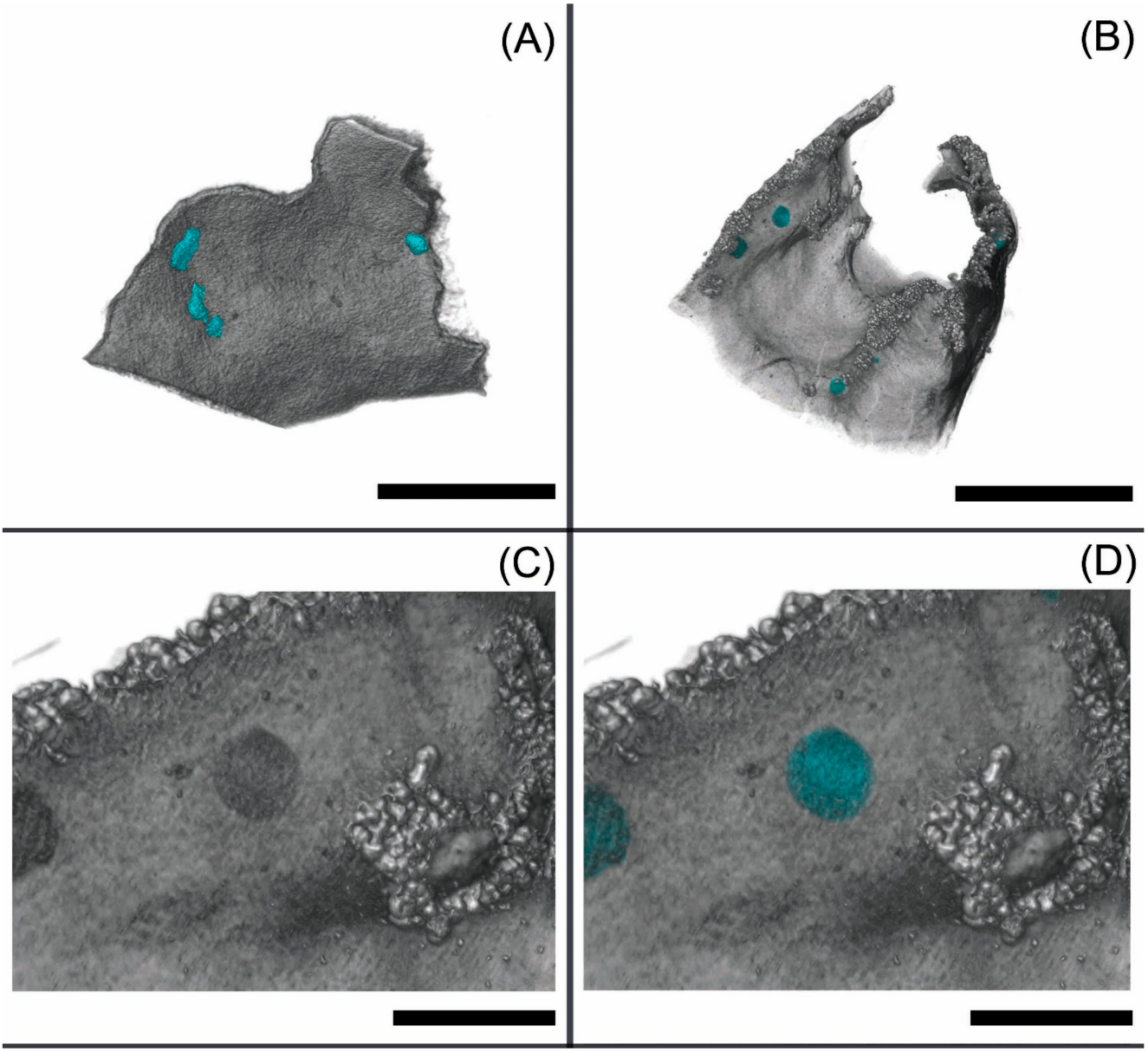

Figure 4. Positions of cephalodia in the lichen thalli after identification using the *Segmentation* tool. (**A**) *Peltigera leucophlebia* (overview, cephalodia coloured). (**B**) *Lobaria pulmonaria* (overview, cephalodia coloured). (**C**) *L. pulmonaria* (close-up, cephalodia uncoloured). (**D**) *L. pulmonaria* (close-up, cephalodia coloured). Internal surfaces are shown in a transparent mode and highlighted in cyan blue in A, B and D. Scale 1 mm (**A**), 2 mm (**B**), and 0.5 mm (**C**,**D**).

2.3.3. Measurements of Segmented Structures Performed by *Label Analysis*

After *Segmentation*, we applied *Label Analysis* to measure the volume of the whole lichen sample and the segmented cephalodia. *Label Analysis* computes a group of measurements on each component (*Material*) of the input *label field* dataset and calculates the resulting values [29], such as *Volume 3D*: Volume of the component (mm^3). After *Label Analysis*, we calculated the cephalodia volume relative to the whole thalli volume.

3. Results

3.1. Morphological Observation

The microCT volumes allowed the detailed observation and examination of both the external and internal components of lichen thalli. The majority of lichens, includ-

ing many crustose species, develop internally stratified thalli: upper cortex, photobiont layer, medulla, and lower cortex [19]. MicroCT resolved the overall structure of all the lichens investigated in this study (Figures 1A,C,E, 2A,C,E and 3). Figure 3 shows virtual sections of the stratified foliose thalli of *Xanthoria parietina* and *Hypogymnia physodes* differentiated in the upper cortex, medulla, and lower cortex. For *Xanthoria parietina*, the structure of the fruiting bodies (apothecia) is discernible in Figures 1A,B and 3A. In *Hypogymnia physodes*, the typical hollow part between the medulla and lower cortex is prominent (Figure 1C,D and Figure 3B). Virtual sections through the foliose *Lobaria pulmonaria* (Figure 1E,F and Figure 3C) and *Peltigera leucophlebia* (Figures 2A,B and 3D) reveal that the lower surfaces of these species are covered by hyphae forming a dense, felt-like, woolly mat, the tomentum. A cross-section through the thallus of the fruticose *Evernia divaricata* shows the characteristic loosely woven medulla (Figures 2C,D and 3F). Figures 2E,F and 3F illustrate a section through the thallus and apothecium of the crustose lichen *Bacidia rubella*.

3.2. Observation of Microstructures

We examined the shape and number of external and internal cephalodia in *Peltigera leucophlebia* and *Lobaria pulmonaria*, respectively. Figure 4A depicts the characteristic appressed, convex, wart-like shaped cephalodia of *P. leucophlebia* with diameters 80–100 × 90–210 µm. We examined ± globose-shaped internal cephalodia in *L. pulmonaria*, with diameters 50–250 × 60–280 µm (Figure 4B–D).

3.3. Segmentation Results and Label Analysis

After the *Segmentation* process, we applied *Label Analysis* to assess the volume of the thalli samples and segmented cephalodia. Subsequently, we calculated the volume of all cephalodia relative to the whole thalli volume.

The *L. pulmonaria* sample had a total volume of 2.091 mm^3 (Table 2) and nine cephalodia of volumes ranging from 0.000046 to 0.004525 mm^3. The total cephalodia volume of 0.153 mm^3 corresponds to 0.73% of the whole thallus volume.

Table 2. *Label Analysis* of the cephalodia of *Lobaria pulmonaria*. *Volume 3D*: Volume of the object (10^{-3} mm^3).

Material	Volume 3D (10^{-3} mm^3)
Whole sample (thallus)	2091
Cephalodium 1	4.525
Cephalodium 2	3.527
Cephalodium 3	3.202
Cephalodium 4	2.913
Cephalodium 5	0.722
Cephalodium 6	0.249
Cephalodium 7	0.059
Cephalodium 8	0.054
Cephalodium 9	0.046
Sum cephalodia	15.30 (0.73%)

The size of the *P. leucophlebia* sample had a total volume of 0.200 mm^3 (Table 3) and four cephalodia of volumes from 0.000201 to 0.000873 mm^3. The total cephalodia volume of 0.0019 mm^3 corresponds to 0.97% of the whole thallus volume.

Table 3. *Label Analysis* of the cephalodia of *Peltigera leucophlebia*. *Volume 3D*: Volume of the object (10^{-3} mm^3).

Material	Volume 3D (10^{-3} mm^3)
Whole sample (thallus)	200
Cephalodium 1	0.873
Cephalodium 2	0.507
Cephalodium 3	0.366
Cephalodium 4	0.201
Sum cephalodia	1.947 (0.97%)

4. Discussion

4.1. Pros and Cons in the Visualisation of Lichens Using MicroCT

Previous studies with microCT applications mainly focused on animal or biomedical data, e.g., references [30–34]. For lichens, examination using X-ray tomography was done very rarely—namely, to estimate the relative mass contribution of lichen symbionts in *Stereocaulon sorediiferum* Hue [35]. MicroCT analysis is a beneficial tool in detailed morphological investigations. For visual examinations, a variety of settings provided by Amira software allow changing or tweaking the appearance of different components of lichen thalli. MicroCT can also be combined with a light microscopic technique [31], complementing the examination of morphological characteristics.

Most importantly, microCT imaging allows the non-destructive exploration of both the external and the internal structures of lichen thalli simultaneously. To this end, we used *Volume Rendering* (*Volren*) by applying the *Grey Colormap*, *VRT*, and *Specular* lighting effects. Moreover, the adjustment of transparency (Figure 4C,D), selective imaging of individual components using *Segmentation* (Figure 4), or clipping off parts of surfaces (Figures 1–3) help to explore the internal lichen structures.

Consequently, a microCT analysis improved the understanding of the structural and functional features of lichens. Separation of the main morphological components depicted in Figures 1–3 (viz., cortex, medulla, and cephalodia) was possible but only related to the fungal component. Thus, the resolution was insufficient to visualise the algal layer with the current setup and depict the algal cells, which appeared as a continuum with the upper cortex. Other approaches, such as staining and embedding (in resin) or applying a higher resolution to smaller thallus areas at microCT acquisition need to be tested for a more detailed examination of the algal cells. These techniques may lead to an enhanced resolution of the microstructure.

Some lichens are very hardy organisms and can even survive conditions in outer space [36]. It is therefore likely that they can withstand the X-ray treatment in the CT instrument and resume growing afterwards. If this proves right, it will pave the way for developmental studies of 3D visualisation of one and the same lichen thallus at different points in time. Lichen developmental studies would greatly benefit from such investigations.

The microCT technique may also advance the knowledge on trapped particles or lichen secondary metabolites—often deposited in crystals—in the thallus. Given the voxel size of 1.25–1.65, particles/crystals larger than 4 µm (2.5× voxel size) can routinely be detected. The MicroCT analysis of these components will be useful for ecological studies investigating the effect of the lichen secondary metabolites, e.g., in herbivory, or the amount of substrate erosion by particle uptake.

4.2. Segmentation and Statistical Analysis of External and Internal Cephalodia

Most cephalodia are morphologically simple globose, sacculate, lobate, or coralloid structures that differ from the rest of the vegetative thallus by their photosynthetic partner and, thus, coloration [19]. The number of cephalodia is ecologically important, because the incorporated cyanobacteria bind atmospheric nitrogen, resulting in a com-

paratively high organic nitrogen content of the lichen thallus and, in consequence, contribute significant amounts of organic nitrogen to forests and, especially, to oligotrophic ecosystems [21–23]. Cornejo and Scheidegger [25] studied the ontogeny of cephalodia structures in *L. pulmonaria*, indicating the active incorporation of the cyanobacteria into the lichen thallus. The application of the *Segmentation* tool allowed us to examine formerly hardly accessible internal cephalodia. Thus, using a microCT analysis, we depicted the form of the internal cephalodia of *L. pulmonaria* for the first time. Our study could clearly demonstrate that *L. pulmonaria* is characterised by having ± globose-shaped internal cephalodia (Figure 4B–D). Moreover, we surveyed the external cephalodia of *P. leucophlebia* as convex and oblong with narrowed ends (so-called peltate cephalodia), which corresponds to previous studies [37].

To further demonstrate the power of the microCT analysis in lichenology, we disclosed the number and distribution of cephalodia within/on the surface of the lichen sample. This was followed by measuring the volume of all cephalodia and their relation to the whole lichen sample (see above). We could clearly demonstrate that the internal cephalodia of *L. pulmonaria* have a volume ranging between 0.046 and 4.5×10^{-3} mm^3. In comparison, volumes of the external *P. leucophlebia* cephalodia are smaller and range between 0.2 and 0.87×10^{-3} mm^3. These data considerably complement our knowledge of the morphological and quantitative characteristics of these lichens.

So far, we have performed a manual *Segmentation* of cephalodia—the most time-consuming step in whole-image processing. Future studies may include automatised (machine learning-based) approaches, which may significantly improve the workflow in terms of efficiency and accuracy. This will allow for the analysis of larger quantities of lichen thalli, facilitating the comparison of lichens grown under different ecological regimes and allowing to investigate the algal layer.

Author Contributions: Conceptualisation, A.B.; formal analysis, J.G.; funding acquisition, A.B.; investigation, J.G.; methodology, B.R. and A.B.; project administration, A.B.; software, B.R.; supervision, B.R. and A.B.; validation, J.G., B.R. and A.B.; writing—original draft, J.G. and A.B.; and writing—review and editing, J.G., B.R. and A.B. All authors have read and agreed to the published version of the manuscript.

Funding: This research was funded by the Staatliche Naturwissenschaftliche Sammlungen Bayerns, grant SNSBinnovativ to A.B.

Institutional Review Board Statement: Not applicable.

Informed Consent Statement: Not applicable.

Data Availability Statement: Not applicable.

Acknowledgments: We thank the government of the administrative district of Swabia for the sampling permit. J.G. was supported by a BAYHOST fellowship from the Bayerische Staatsministerium für Bildung und Kultus, Wissenschaft und Kunst.

Conflicts of Interest: The authors declare no conflict of interest.

Ethical Statements: The lichens used in this study were collected in Bavaria, Germany. *Bacidia rubella*, *Evernia divaricata*, *Hypogymnia physodes*, *Lobaria pulmonaria*, and *Peltigera leucophlebia* were collected under permit 55.3-8645-2/35 of the government of the administrative district of Swabia. *Xanthoria parietina* was collected in Upper Bavaria outside protected areas, and thus, no permit was required. Voucher specimens were deposited in the Botanische Staatssammlung München under the herbarium numbers given in the Materials and Methods section.

References

1. Ruthensteiner, B. Soft Part 3D visualisation by serial sectioning and computer reconstruction. *Zoosymposia* **2008**, *1*, 61–100. [CrossRef]
2. Handschuh, S.; Baeumler, N.; Schwaha, T.; Ruthensteiner, B. A correlative approach for combining microCT, light and transmission electron microscopy in a single 3D scenario. *Front. Zool.* **2013**, *10*, 44. [CrossRef] [PubMed]

3. Farrar, J.F. The lichen as an ecosystem: Observation and experiment. In *Lichenology: Progress and Problems*; Brown, D.H., Hawksworth, D.L., Bailey, R.H., Eds.; Academic Press: London, UK, 1976; pp. 385–406.
4. Werth, S. How does the lichen symbiosis work? Journey into the unknown. *Fritschiana* **2017**, *85*, 48–49.
5. Mark, K.; Laanisto, L.; Bueno, C.G.; Niinemets, Ü.; Keller, C.; Scheidegger, C. Contrasting co-occurrence patterns of photobiont and cystobasidiomycete yeast associated with common epiphytic lichen species. *New Phytol.* **2020**, *227*, 1362–1375. [CrossRef]
6. Tzovaras, B.G.; Segers, F.H.I.D.; Bicker, A.; Dal Grande, F.; Otte, J.; Anvar, S.Y.; Hankeln, T.; Schmitt, I.; Ebersberger, I. What is in *Umbilicaria pustulata*? A metagenomic approach to reconstruct the holo-genome of a lichen. *Genome Biol. Evol.* **2020**, *12*, 309–324. [CrossRef] [PubMed]
7. Grube, M. Lichens growing greenhouses en miniature. *Microbial Cell* **2021**, *8*, 65–68. [CrossRef] [PubMed]
8. Honegger, R. The Symbiotic Phenotype of Lichen-Forming Ascomycetes and Their Endo- and Epibionts. In *The Mycota IX—Fungal Associations*; Hock, B., Ed.; Springer: Berlin/Heidelberg, Germany, 2012; pp. 287–339.
9. Büdel, B.; Scheidegger, C. Thallus morphology and anatomy. In *Lichen Biology*; Nash, T.H., III, Ed.; Cambridge University Press: Cambridge, UK, 1996; pp. 24–36.
10. Eisenreich, W.; Knispel, N.; Beck, A. Advanced methods for the study of the chemistry and the metabolism of lichens. *Phytochem. Rev.* **2011**, *10*, 445–456. [CrossRef]
11. Kuhn, V.; Geisberger, T.; Huber, C.; Beck, A.; Eisenreich, W. A facile in vivo procedure to analyse metabolic pathways in intact lichens. *New Phytol.* **2019**, *224*, 1657–1667. [CrossRef]
12. Singh, G.; Grande, F.D.; Divakar, P.K.; Otte, J.; Leavitt, S.D.; Szczepańska, K.; Crespo, A.; Rico, V.J.; Aptroot, A.; Cáceres, M.E.D.S.; et al. Coalescent–based species delimitation approach uncovers high cryptic diversity in the cosmopolitan lichen–forming fungal genus *Protoparmelia* (Lecanorales, Ascomycota). *PLoS ONE* **2015**, *10*, e0124625. [CrossRef]
13. Altermann, S.; Leavitt, S.D.; Goward, T.; Nelsen, M.P.; Lumbsch, H.T. How do you solve a problem like *Letharia*? A new look at cryptic species in lichen-forming fungi using Bayesian clustering and SNPs from multilocus sequence data. *PLoS ONE* **2014**, *9*, e97556. [CrossRef]
14. Kraichak, E.; Lücking, R.; Aptroot, A.; Beck, A.; Dornes, P.; John, V.; Lendemer, J.C.; Nelsen, M.P.; Neuwirth, G.; Nutakki, A.; et al. Hidden diversity in the morphologically variable script lichen (*Graphis scripta*) complex (Ascomycota, Ostropales, Graphidaceae). *Org. Divers. Evol.* **2015**, *15*, 447–458. [CrossRef]
15. Frolov, I.; Vondrák, J.; Fernández-Mendoza, F.; Wilk, K.; Khodosovtsev, A.; Halici, H.G. Three new, seemingly–cryptic species in the lichen genus *Caloplaca* (Teloschistaceae) distinguished in two–phase phenotype evaluation. *Ann. Bot. Fenn.* **2016**, *53*, 243–262. [CrossRef]
16. Leavitt, S.D.; Esslinger, T.L.; Divakar, P.K.; Crespo, A.; Lumbsch, H.T. Hidden diversity before our eyes: Delimiting and describing cryptic lichen-forming fungal species in camouflage lichens (Parmeliaceae, Ascomycota). *Fungal Biol.* **2016**, *120*, 1374–1391. [CrossRef]
17. Boluda, C.G.; Rico, V.J.; Divakar, P.K.; Nadyeina, O.; Myllys, L.; McMullin, R.T.; Zamora, J.C.; Scheidegger, C.; Hawksworth, D.L. Evaluating methodologies for species delimitation: The mismatch between phenotypes and genotypes in lichenised fungi (Bryoria sect. Implexae, Parmeliaceae). *Persoonia* **2019**, *42*, 75–100. [CrossRef]
18. Del-Prado, R.; Buaruang, K.; Lumbsch, H.T.; Crespo, A.; Divakar, P.K. DNA sequence-based identification and barcoding of a morphologically highly plastic lichen forming fungal genus (*Parmotrema*, Parmeliaceae) from the tropics. *Bryologist* **2019**, *122*, 281–291. [CrossRef]
19. Nash, T.H. (Ed.) *Lichen Biology*, 2nd ed.; Cambridge University Press: Cambridge, UK, 2008.
20. Lawrey, J.D. Biological role of lichen substances. *Bryologist* **1986**, *89*, 111–122. [CrossRef]
21. Knops, J.M.H.; Nash, T.H., III; Boucher, V.L.; Schlesinger, W.H. Mineral cycling and epiphytic lichens: Implications at the ecosystem level. *Lichenologist* **1991**, *23*, 309–321. [CrossRef]
22. Knowles, R.D.; Pastor, J.; Biesboer, D.D. Increased soil nitrogen associated with dinitrogen-fixing, terricolous lichens of the genus *Peltigera* in northern Minnesota. *Oikos* **2006**, *114*, 37–48. [CrossRef]
23. Asplund, J.; Wardle, D.A. How lichens impact on terrestrial community and ecosystem properties. *Biol. Rev.* **2017**, *92*, 1720–1738. [CrossRef] [PubMed]
24. Rose, F.; Purvis, O.W. Lobaria (Schreb.) Hoffm. 1796. In *Lichens of Great Britain and Ireland*; Smith, C.W., Aptroot, A., Coppins, B.J., Fletcher, A., Gilbert, O.L., James, P.W., Wolseley, P.A., Eds.; MPG Books Group: London, UK, 2009; pp. 560–562.
25. Cornejo, C.; Scheidegger, C. New morphological aspects of cephalodium formation in the lichen *Lobaria pulmonaria* (Lecanorales, Ascomycota). *Lichenologist* **2013**, *45*, 77–87. [CrossRef]
26. Škaloud, P.; Friedl, T.; Hallmann, C.; Beck, A.; Dal Grande, F. Taxonomic revision and species delimitation of coccoid green algae currently assigned to the genus *Dictyochloropsis* (Trebouxiophyceae, Chlorophyta). *J. Phycol.* **2016**, *52*, 599–617. [CrossRef]
27. Grimm, M.; Grube, M.; Schiefelbein, U.; Zühlke, D.; Bernhardt, J.; Riedel, K. The Lichens' Microbiota, Still a Mystery? *Front. Microbiol.* **2021**, *12*, 623839. [CrossRef] [PubMed]
28. Metscher, B.D. MicroCT for developmental biology: A versatile tool for high-contrast 3D imaging at histological resolutions. *Dev. Dyn.* **2009**, *238*, 632–640. [CrossRef]
29. Thermo Scientific. *User's Guide Amira Software 2019*. Available online: https://assets.thermofisher.com/TFS-Assets/MSD/Product-Guides/users-guide-amira-software-2019.pdf (accessed on 9 March 2021).

30. Handschuh, S.; Beisser, C.J.; Ruthensteiner, B.; Metscher, B.D. Microscopic dual-energy CT (microDECT): A flexible tool for multichannel ex vivo 3D imaging of biological specimens. *J. Microsc.* **2017**, *67*, 3–26. [CrossRef] [PubMed]
31. Karreman, M.A.; Ruthensteiner, B.; Mercier, L.; Schieber, N.L.; Solecki, G.; Winkler, F.; Goetz, J.G.; Schwab, Y. Find your way with X-Ray: Using microCT to correlate in vivo imaging with 3D electron microscopy. *Methods Cell Biol.* **2017**, *140*, 277–301. [PubMed]
32. Jacob, D.E.; Ruthensteiner, B.; Trimby, P.; Henry, H.; Martha, S.O.; Leitner, J.; Otter, L.M.; Scholz, J. Architecture of *Anoteropora latirostris* (Bryozoa, Cheilostomata) and implications for their biomineralisation. *Sci. Rep.* **2019**, *9*, 11439. [CrossRef]
33. Schwaha, T.; Ruthensteiner, B.; Melzer, R.R.; Asami, T.; Páll-Gergely, B. Three phyla—Two type specimens—One shell: History of a snail shell revealed by modern imaging technology. *J. Zool. Syst. Evol. Res.* **2019**, *57*, 527–533. [CrossRef]
34. Orhan, K. (Ed.) *Micro-Computed Tomography (micro-CT) in Medicine and Engineering*; Springer: Berlin/Heidelberg, Germany, 2020.
35. Kosugi, M.; Shizuma, R.; Moriyama, Y.; Koike, H.; Fukunaga, Y.; Takeuchi, A.; Uesugi, K.; Suzuki, Y.; Imura, S.; Kudoh, S.; et al. Ideal osmotic spaces for chlorobionts or cyanobionts are differentially realized by lichenized fungi. *Plant Physiol.* **2014**, *166*, 337–348. [CrossRef]
36. Brandt, A.; de Vera, J.P.; Onofri, S.; Ott, S. Viability of the lichen *Xanthoria elegans* and its symbionts after 18 months of space exposure and simulated mars conditions on the ISS. *Int. J. Astrobiol.* **2015**, *14*, 411–425. [CrossRef]
37. Goward, T.; Goffinet, B.; Vitikainen, O. Synopsis of the genus *Peltigera* (lichenized Ascomycetes) in British Columbia, with a key to the North American species. *Canad. J. Bot.* **1995**, *73*, 91–111. [CrossRef]